AIP | APL Materials

Upper limit of the electrocaloric peak in lead-free ferroelectric relaxor ceramics

Florian Le Goupil and Neil McN. Alford

Citation: APL Mater. **4**, 064104 (2016); doi: 10.1063/1.4950790
View online: http://dx.doi.org/10.1063/1.4950790
View Table of Contents: http://scitation.aip.org/content/aip/journal/aplmater/4/6?ver=pdfcov
Published by the AIP Publishing

Upper limit of the electrocaloric peak in lead-free ferroelectric relaxor ceramics

Florian Le Goupil[a] and Neil McN. Alford
Department of Materials, Imperial College London, London SW7 2AZ, United Kingdom

(Received 27 February 2016; accepted 29 April 2016; published online 17 May 2016)

The electrocaloric effect (ECE) of two compositions (x = 0.06 and 0.07) of $(1 - x)(Na_{0.5}Bi_{0.5})TiO_3$-$xKNbO_3$ in the vicinity of the morphotropic phase boundary is studied by direct measurements. ΔT_{max} = 1.5 K is measured at 125 °C under 70 kV/cm for NBT-6KN while ΔT_{max} = 0.8 K is measured at 75 °C under 55 kV/cm for NBT-7KN. We show that the "shoulder," T_S, in the dielectric permittivity, marks the upper limit of the ECE peak under high applied electric fields. These results imply that the range of temperature with high ECE can be quickly identified for a given composition, which will significantly speed up the process of materials selection for ECE cooling.
[http://dx.doi.org/10.1063/1.4950790]

The need for more efficient and environmentally friendly materials in the refrigeration industry has led to a significant effort towards the discovery of materials with potential for solid state cooling. Adiabatic depolarization cooling, which is based on the electrocaloric effect (ECE), is a promising contender for new solid state refrigeration techniques. In polar crystals, net polarization increases under an external electric field. Under adiabatic conditions, the system compensates this alignment of dipoles with an increase in temperature keeping the entropy of the system constant.[1,2] This phenomenon is the electrocaloric effect (ECE).[3–7] Lead-free relaxor ferroelectrics with high dielectric strength[8] are suitable candidates for solid state refrigeration, due to the extra contribution of their polar nano-regions (PNRs); however, their ECE must be increased. One approach is to operate close to critical points (CPs) where energy barriers for switching between different phases are reduced. As more than one polar phase coexist near the CP, the entropy of this region is increased. This leads to ECE enhancement,[9] as reported by Qian *et al.* in Zr-doped $BaTiO_3$(BT).[10] It has been shown that an invariant CP, where the number of polar phases in the composition-temperature-electric field phase diagram is maximised, is found in materials with a MPB, as observed in $(1 - x)Pb(Mg_{1/3}Nb_{2/3})O_3$-$xPbTiO_3$ (PMN-xPT) with $x \sim 0.30$.[11,12] $(Na_{0.5}Bi_{0.5})TiO_3$ (NBT) forms solid solutions with numerous ferroelectric materials, such as BT or $(K_{0.5}Bi_{0.5})TiO_3$ (KBT) and several MPB have been reported.[13,14] The highest electromechanical properties, including the ECE[15,16] for NBT-BT and NBT-KBT, were reported near the MPB. However, the temperature of depolarization (Td) in these systems occurs above 100 °C. As the electrocaloric peak is observed near Td, it is essential to find ways to shift it closer to room temperature (RT) where it is required for application in commercial household refrigerators. Several A-sites and B-sites substitutions have been attempted, but in most cases, a strong field-dependence of the position of the electrocaloric peak was induced.[16] Although the low-field ECE peak was indeed shifted closer to RT, the reverse trend was observed for the high-field ECE peak, which sometimes moved more than 100 °C above Td. The inability to predict the position of the ECE maximum makes the choice of materials very difficult and implies that a systematic characterisation of each composition is required, which can be time-consuming.

[a]Electronic mail: f.le-goupil09@imperial.ac.uk

Here we report the direct ECE characterisation of two compositions (x = 0.06 and 0.07) of $(1-x)(Na_{0.5}Bi_{0.5})TiO_3$-$xKNbO_3$ in the vicinity of the MPB. (1 − x)NBT-xKN will be denoted as NBT-100xKN.

The NBT-KN ceramic powders were prepared by conventional solid-state synthesis. Stoichiometric quantities of the starting reagents, Bi_2O_3, K_2CO_3, Na_2CO_3, N_2O_5, and TiO_2 (99.9% purity, Sigma-Aldrich) were mixed in a ball mill for 24 h then dried. The powders were calcined in covered crucibles at 900 °C for 5 h. The calcined powders were subject to high energy attrition milling to reduce the particle size for 2 h with stabilized yttria stabilized zirconia balls in iso-propyl alcohol. The calcined powders were pressed into 5 mm-diameter pellets and sintered at 1150 °C for 2 h in covered crucibles. The ceramic pellets were polished down to a thickness of 0.4 mm. Densities corresponding to 97% and 96% of the theoretical values were obtained for NBT-6KN and NBT-7KN, respectively. The dielectric permittivity was measured with a HP 4263B LCR meter from 25 °C to 450 °C at different frequencies (from 1 kHz to 100 kHz) on both poled and unpoled ceramics. The samples were poled under high electric field (50 kV/cm) at 50 °C for NBT-6KN and at 25 °C for NBT-7KN. The polarization versus electric field measurements (*P*-*E*), along with leakage current measurements, were carried out using a Radiant LC Precision Unit with a high voltage amplifier (TREK model 609B) from 20 °C to 145 °C. The specific heat capacities of NBT-6KN and NBT-7KN were measured experimentally and were found to linearly increase over the studied temperature range from 579 to 591 J kg^{-1} K^{-1}, and from 548 to 554 J kg^{-1} K^{-1}, respectively. The direct ECE measurements were performed on the poled ceramics with a modified-differential scanning calorimeter (Netzsch DSC 200 F3), as described elsewhere.[5]

Fig. 1 shows the real part of the dielectric permittivity and the loss tangent as a function of temperature measured for (a) NBT-6KN and (b) NBT-7KN poled ceramics measured at three different frequencies upon heating. The shape of the plots is typical of the NBT-based system, with two successive dielectric anomalies, T_S and Tm. T_S is used to describe the "shoulder"-like low temperature anomaly. Similarly to NBT-06BT,[16,17] the low temperature phase consists of a mixture of polar nano-regions (PNRs) with two different local symmetries, rhombohedral (*R*3*c*) and tetragonal (*P*4*bm*) in a cubic matrix. Upon heating through T_S, the mixture of randomly oriented slowed-down PNRs starts undergoing rapid thermal fluctuations.[18] The higher temperature anomaly, Tm, is the convolution of two distinct processes: the diffuse phase transition of lower symmetry PNRs (*R*3*c*) into higher symmetry PNRs (*P*4*bm*), and the additional dielectric relaxation of existing PNRs.[17,19] T_S was measured at ~129 °C for NBT-6KN. The "shoulder"-like shape near T_S can make its estimation difficult. In this work, we used the intersection of two tangents as shown in the inset of Fig. 1(b). As expected from the literature,[20] T_S shifts to lower temperature when the KN content is increased, with T_S ~ 101 °C for NBT-7KN. The frequency dispersion observed for both compositions near T_S suggests relaxor-type properties, which arise from the A-site cation disorder

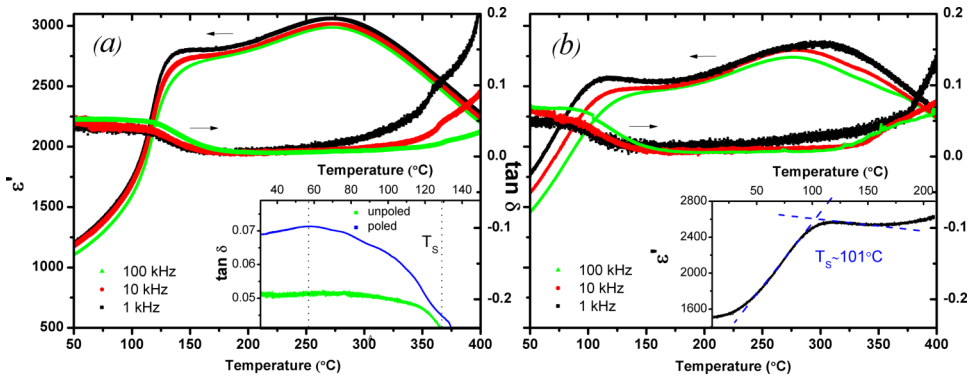

FIG. 1. Real part of the dielectric permittivity and loss tangent as a function of temperature measured for (a) NBT-6KN and (b) NBT-7KN poled ceramics measured at three different frequencies upon heating. The insets show (a) the loss tangent versus temperature for poled and unpoled NBT-6KN ceramics at 100 kHz and (b) a close-up of the "shoulder" measured at 1 KHz on the NBT-7KN poled ceramic.

and should lead to a strong field-dependence of the position of the ECE peak. In some cases, a third anomaly, consisting of a sharp change in permittivity, can be observed below T_S for poled samples. This anomaly marks the temperature of depolarization Td, sometimes also called T_{F-R}. This corresponds to the temperature where the long-range ferroelectric order induced by the poling reverts back to the initial weakly polar relaxor state upon heating due to thermal fluctuations. Although Td is easy to identify on the permittivity data for conventional ferroelectrics, it is significantly more difficult for relaxors due to the more diffused process involved. A comparison of loss tangent data measured on both poled and unpoled samples, as shown in the inset of Fig. 1(a) for NBT-6KN, can provide more information. The shape of the loss tangent data for the poled samples suggests that the depolarization process occurs between 57 °C and 129 °C, but a more accurate value of Td is not available. The comparison of the loss data for poled and unpoled samples can also help identify T_S, which occurs when the two sets of data superimpose at ~130 °C for NBT-6KN.

Fig. 2 shows the polarization as a function of the applied electric field and temperature for (a) NBT-6KN and (b) NBT-7KN poled ceramics. A significant drop of the remanent polarization is observed in the insets for both compositions. The onset of depolarization occurs at ~50 °C for NBT-6KN and ~40 °C for NBT-7KN. The temperature of the steepest decrease of remanent polarization corresponds to Td, which is found at 78 °C for NBT-6KN and 53 °C for NBT-7KN. As expected, Td shifts to lower temperature when the KN content is increased.[20] Using a formula proposed by Hiruma *et al.*,[21] which allows the prediction of the MPB composition as a function of the tolerance factor of the perovskite ABO_3 in NBT-ABO_3 solid solutions, we estimated the MPB composition to be between NBT-7KN and NBT-8KN. As the composition approaches the MPB, Td and T_S start to converge until they superimpose. The temperature gap between Td and T_S in both studied compositions indicates that the MPB is not reached. Furthermore, the fact that this gap is slightly wider in NBT-6KN (51 °C) than in NBT-7KN (48 °C) implies that NBT-7KN is closer to the MPB composition, which is in good agreement with our prediction of the MPB being found at higher KN contents. Fig. 2(a) also shows a constriction in the polarization hysteresis loops measured above Td. This constriction has been wrongly attributed to an antiferroelectric phase in the past,[13] but it actually corresponds to the previously mentioned field induced phase transition from weakly polar relaxor to ferroelectric. Above Td, the ferroelectric long range order can no longer be maintained. The ferroelectric phase can still be induced by the application of a strong enough electric field but the system reversibly reverts back to the relaxor phase when the field is removed, which is the reason for this "AFE-like" constricted polarization hysteresis loop.

Fig. 3 shows the ECE versus temperature obtained by direct measurements for several values of applied electric field for the (a) NBT-6KN and (b) NBT-7KN poled ceramics. A strong field dependence is observed for both compositions, with the temperature of maximum ECE, ΔT_{max}, shifting to significantly higher temperature when a stronger field is applied. For NBT-6KN, $\Delta T_{max} \sim 0.3$ K is measured at 75 °C under 30 kV/cm, while $\Delta T_{max} \sim 1.5$ K under 70 kV/cm is measured at

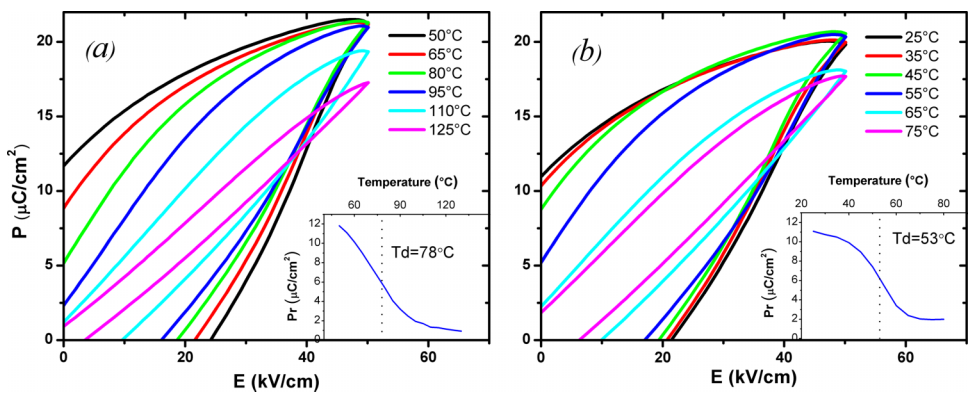

FIG. 2. Polarization as a function of the applied electric field and temperature for (a) NBT-6KN and (b) NBT-7KN poled ceramics measured at 10 Hz. The insets show the remanent polarization versus temperature.

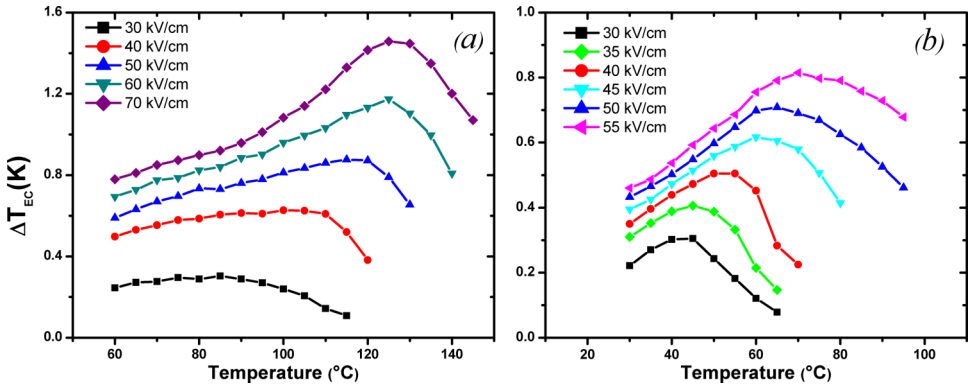

FIG. 3. ECE versus temperature obtained by direct measurements for several values of applied electric field for the (a) NBT-6KN and (b) NBT-7KN poled ceramics.

125 °C. In the case of NBT-7KN, $\Delta T_{max} \sim 0.3$ K is measured at 45 °C under 30 kV/cm, while $\Delta T_{max} \sim 0.8$ K under 55 kV/cm is measured at 70 °C. Unfortunately, 70 kV/cm could not be applied to the NBT-7KN ceramics without inducing significant leakage currents which prevented reliable ECE measurements. Such a strong field dependence has been previously observed in doped-NBT ceramics for non-MPB compositions.[15,16] It tends to decrease when the compositional changes bring the system closer to the MPB. The field dependence seems less pronounced for NBT-7KN, which would imply that this composition is closer to the MPB and is in good agreement with our prediction that the MPB is found at higher KN contents. The ECE responsivity, $\Delta T_{max}/\Delta E$, is often used to compare performances of ECE materials in the literature. The ECE responsivity must be used with caution as it has been shown that it is not a constant function of the applied electric field,[15] but it is a useful comparison tool. The ECE responsivity was found to be 0.21×10^{-6} K m/V for NBT-6KN and 0.15×10^{-6} K m/V for NBT-7KN. These values are low when compared with the best lead free ceramics ($>0.3 \times 10^{-6}$ K m/V[10,15,16]), which emphasises the need to work at the MPB composition where the best ECE responsivities are found.[16]

Fig. 4(a) shows the real part of the permittivity at 1 kHz and the ECE at 30 kV/cm (red) and 70 kV/cm (blue) versus temperature for NBT-6KN. At low fields, the ECE starts increasing near the onset of depolarization (~50 °C) and reaches a maximum value at Td, then it slowly decreases until it reaches zero near Ts. As previously mentioned, no noticeable change is observed near Td in the dielectric permittivity data. However, at high fields, the ECE increases continuously through Td until it reaches its maximum near T_S. Fig. 4 shows that there is good match between the

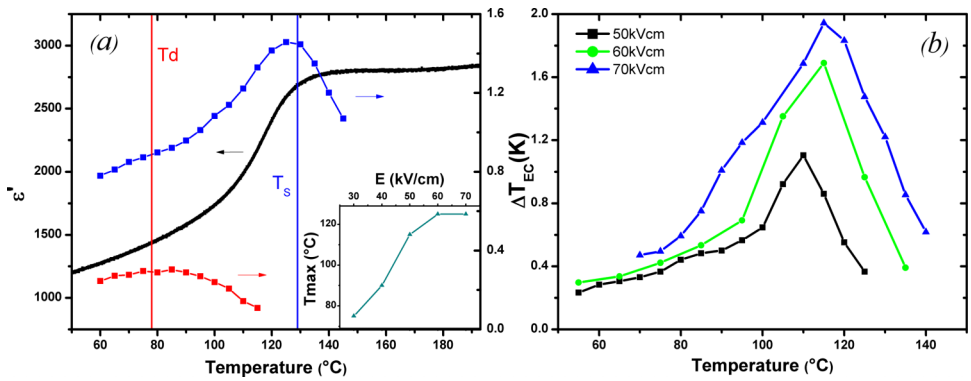

FIG. 4. (a) Real part of the permittivity at 1 kHz and ECE at 30 kV/cm (red) and 70 kV/cm (blue) versus temperature for NBT-6KN. The inset shows the evolution of the temperature of the maximum ECE as a function of applied electric field. (b) ECE versus temperature for three different applied electric fields obtained by indirect estimation from P(T,E) data measured on NBT-6KN.

temperature of maximum ECE at high fields and T_S. High polarizations values can still be obtained above Td if a high enough field is applied to induce the relaxor-to-ferroelectric phase transition. However, when Ts is reached, the thermal fluctuations make the establishment of the ferroelectric phase difficult, even under high fields, which leads to a decrease of the maximum polarization (P_{max}) with temperature. This fast change of P_{max} with temperature is responsible for the ECE peak observed near Ts at high fields. Fig. 4(b) shows the ECE versus temperature for three different applied electric fields obtained by indirect estimation from P(T,E) data measured on NBT-6KN. The indirect EC temperature change (ΔT_{EC}) at a temperature T_n was calculated from the following equation, where C and ρ are the specific heat capacity and density of the material at T_n, respectively: $\Delta T_{EC} = \frac{1}{\rho C}\int_{E1}^{E2} T_n(\partial P/\partial T)_E dE$, assuming the Maxwell relation $(\partial P/\partial T)_E = (\partial S/\partial E)_T$.[8] As expected, there are discrepancies between direct and indirect absolute values of ECE. The indirect method seems to overestimate the ECE near maximum, with $\Delta T_{max} \sim 1.9$ K for 70 kV/cm compared with $\Delta T_{max} \sim 1.5$ K for direct measurements, and underestimate values away from the peak, with the indirect $\Delta T_{EC}(75\,^{\circ}C) \sim 0.5$ K compared with $\Delta T_{EC}(75\,^{\circ}C) \sim 0.9$ K for direct measurements at 70 kV/cm. However, Fig. 4(b) also shows that there is a good match between both methods when comparing the position of the ECE peak at high fields. The maximum ECE is observed a few tens of degrees below T_S at 50 kV/cm and the peak shifts closer to Ts when stronger fields are applied, with ΔT_{max} measured at 115 °C for 70 kV/cm, which is just 10 °C below the peak position obtained by direct measurements. These results show that, although it must be used with caution as only direct measurements can provide reliable values of ECE, the indirect method can be used to predict the position of ΔT_{max} and the trend of the ECE versus field and temperature. However, this method seems only valid in doped-NBT systems when working above Td as shown in our previous work on NBT-KBT.[16]

This work is the first direct observation of the role of T_S in the position of the ECE peak. Previous studies have mainly focused on measuring the ECE in the vicinity of Td[22] but no reports of direct measurements near T_S can be found in the literature with the exception of MPB compositions such as NBT-06BT.[16] At the MPB, Td and T_S are superimposed, which makes any conclusions on the individual role of each of these temperatures impossible. These results show that a fast screening of potential candidates for ECE cooling can be done by simply measuring the dielectric permittivity versus temperature and the P(T,E). The dielectric data allow for an easy identification of T_S, which can be used to predict the position of the ECE peak at high fields. The P(T,E) data provide the temperatures involved in the depolarization process, which can be used to predict the onset of the ECE peak and the temperature of the maximum ECE at low fields.

In conclusion, we have reported direct measurements of the ECE for two compositions of NBT-KN in the vicinity of the MPB. $\Delta T_{max} = 1.5$ K was measured at 125 °C under 70 kV/cm for NBT-6KN and $\Delta T_{max} = 0.8$ K was measured at 75 °C under 55 kV/cm for NBT-7KN. The low corresponding ECE responsivities indicated that a higher KN concentration needs to be introduced to the system to obtain the MPB composition in NBT-KN, which was confirmed by the permittivity and polarization versus temperature data. Comparisons of the ECE data with the dielectric permittivity measurements have shown that T_S plays a major role in the position of the ECE peak under high applied electric fields. These results imply that the range of temperature with high ECE can be quickly identified for a given composition of a NBT-based material, by simply measuring the dielectric permittivity and the polarization versus temperature and electric field, which will significantly speed up the process of materials selection for ECE cooling.

This project was funded by the EPSRC (Grant No. EP/G060940/1) and the Royal Society.

[1] T. Correia and Q. Zhang, *Electrocaloric Materials* (Springer, Berlin, Heidelberg, 2014).
[2] U. Plaznik, A. Kitanovski, B. Rožič, B. Malič, H. Uršič, S. Drnovšek, J. Cilenšek, M. Vrabelj, A. Poredoš, and Z. Kutnjak, Appl. Phys. Lett. **106**, 043903 (2015).
[3] M. Valant, Prog. Mater. Sci. **57**, 980 (2012).
[4] A. S. Mischenko, Q. Zhang, J. F. Scott, R. W. Whatmore, and N. D. Mathur, Science **311**, 1270 (2006).
[5] F. Le Goupil, A. Berenov, A.-K. Axelsson, M. Valant, and N. M. Alford, J. Appl. Phys. **111**, 124109 (2012).
[6] X. Moya, E. Stern-Taulats, S. Crossley, D. González-Alonso, S. Kar-Narayan, A. Planes, L. Mañosa, and N. D. Mathur, Adv. Mater. **25**, 1360 (2013).

[7] F. Le Goupil, A.-K. Axelsson, L. J. Dunne, M. Valant, G. Manos, T. Lukasiewicz, J. Dec, A. Berenov, and N. M. Alford, Adv. Energy Mater. **4**, 1301688 (2014).
[8] M. Valant, A.-K. Axelsson, F. Le Goupil, and N. M. Alford, Mater. Chem. Phys. **136**, 277 (2012).
[9] Z. K. Liu, X. Li, and Q. M. Zhang, Appl. Phys. Lett. **101**, 082904 (2012).
[10] X.-S. Qian, H.-J. Ye, Y.-T. Zhang, H. Gu, X. Li, C. A. Randall, and Q. M. Zhang, Adv. Funct. Mater. **24**, 1300 (2014).
[11] Z. Kutnjak, J. Petzelt, and R. Blinc, Nature **441**, 956 (2006).
[12] Z. Kutnjak, R. Blinc, and Y. Ishibashi, Phys. Rev. B **76**, 104102 (2007).
[13] Y. Hiruma, H. Nagata, and T. Takenaka, J. Appl. Phys. **104**, 124106 (2008).
[14] S.-T. Zhang, A. B. Kounga, W. Jo, C. Jamin, K. Seifert, T. Granzow, J. Rodel, and D. Damjanovic, Adv. Mater. **21**, 4716 (2009).
[15] F. Le Goupil, J. Bennett, A.-K. Axelsson, M. Valant, A. Berenov, A. J. Bell, T. P. Comyn, and N. M. Alford, Appl. Phys. Lett. **107**, 172903 (2015).
[16] F. Le Goupil, R. McKinnon, V. Koval, G. Viola, S. Dunn, A. Berenov, H. Yan, and N. M. Alford, "Tuning the electrocaloric enhancement near the morphotropic phase boundary in lead-free ceramics," Sci. Rep. (submitted).
[17] W. Jo, S. Schaab, E. Sapper, L. A. Schmitt, H.-J. Kleebe, A. J. Bell, and J. Rödel, J. Appl. Phys. **110**, 074106 (2011).
[18] G. A. Samara, J. Phys.: Condens. Matter **15**, R367 (2003).
[19] W. Jo, R. Dittmer, M. Acosta, J. Zang, C. Groh, E. Sapper, K. Wang, and J. Rödel, J. Electroceram. **29**, 71 (2012).
[20] X. Jiang, L. Luo, B. Wang, W. Li, and H. Chen, Ceram. Int. **40**, 2627 (2014).
[21] Y. Hiruma, H. Nagata, and T. Takenaka, Jpn. J. Appl. Phys., Part 1 **48**, 09KC08 (2009).
[22] J. Hagberg, M. Dunce, E. Birks, M. Antonova, and A. Sternberg, Ferroelectrics **428**, 20 (2012).